Graefe's Archive for Clinical and Experimental Ophthalmology (2021) 259:1803–1809
https://doi.org/10.1007/s00417-021-05104-4

RETINAL DISORDERS

Classification of pachychoroid on optical coherence tomography using deep learning

Nam Yeo Kang[1] · Ho Ra[1] · Kook Lee[2] · Jun Hyuk Lee[1] · Won Ki Lee[3] · Jiwon Baek[1]

Received: 12 November 2020 / Revised: 11 January 2021 / Accepted: 26 January 2021 / Published online: 22 February 2021
© The Author(s), under exclusive licence to Springer-Verlag GmbH, DE part of Springer Nature 2021

Abstract

Purpose Pachychoroid is characterized by dilated Haller vessels and choriocapillaris attenuation that are seen on optical coherence tomography (OCT) B-scans. This study investigated the feasibility of using deep learning (DL) models to classify pachychoroid and non-pachychoroid eyes from OCT B-scan images.

Methods In total, 1898 OCT B-scan images were collected from eyes with macular diseases. Images were labeled as pachychoroid or non-pachychoroid based on strict quantitative and qualitative criteria for multimodal imaging analysis by two retina specialists. DL models were trained (80%) and validated (20%) using pretrained convolutional neural networks (CNNs). Model performance was assessed using an independent test set of 50 non-pachychoroid and 50 pachychoroid images.

Results The final accuracy of AlexNet and VGG-16 was 57.52% for both models. ResNet50, Inception-v3, Inception-ResNet-v2, and Xception showed a final accuracy of 96.31%, 95.25%, 93.40%, and 92.61%, respectively, for the validation set. These models demonstrated accuracy on an independent test set of 78.00%, 86.00%, 90.00%, and 92.00%, and an F1 score of 0.718, 0.841, 0.894, and 0.920, respectively.

Conclusion DL models classified pachychoroid and non-pachychoroid images with good performance. Accurate classification can be achieved using CNN models with deep rather than shallow neural networks.

Keywords Pachychoroid · Artificial intelligence · Optical coherence tomography · Convolutional neural network · CSC · PCV · AMD

Nam Yeo Kang and Ho Ra contributed equally to this work.

This article is part of a topical collection on Breakthroughs in artificial intelligence for ophthalmology.

✉ Jiwon Baek
md.jiwon@gmail.com

[1] Department of Ophthalmology, Bucheon St. Mary's Hospital, College of Medicine, The Catholic University of Korea, Gyeonggi-do, Republic of Korea

[2] Department of Ophthalmology, Seoul St. Mary's Hospital, College of Medicine, The Catholic University of Korea, Seoul, Republic of Korea

[3] Retina Division, Nune Eye Center, Seoul, Republic of Korea

Key messages

- The characteristic morphology of pachychoroid of pathologically dilated Haller vessels and choriocapillaris attenuation is well observed by OCT B-scans.
- Artificial intelligence has been applied to many areas of retinal imaging and this study assessed the feasibility of automatic classification of pachychoroid using deep learning.
- Deep learning models classified pachychoroid and non-pachychoroid images with good performance.

Introduction

It has long been suggested that choroidal circulatory disturbance plays a significant pathophysiologic role in some macular diseases. The characteristic indocyanine green angiography (ICGA) findings of choroidal hyperpermeability and dilated choroidal vessels in central serous chorioretinopathy (CSC) have provided this evidence since the 1980s and 1990s [1]. Advances in imaging have enabled better description of the choroidal features of macular diseases that include CSC, polypoidal choroidal vasculopathy, and typical age-related macular degeneration (AMD). In 2013, Warrow et al. [2] described a thickened choroid on enhanced depth imaging (EDI) OCT with overlying retinal pigment epithelium (RPE) abnormalities in eyes with CSC "forme fruste" and the term "pachychoroid" has been coined to encompass a spectrum of diseases that show this characteristic choroid morphology [2, 3]. Associated studies expended the definition of the pachychoroid phenotype to include pachychoroid pigment epitheliopathy, pachychoroid neovasculopathy (PNV), and PCV (polypoidal choroidal vasculopathy) [3–5].

The peculiar morphology of pachychoroid of pathologically dilated Haller vessels (i.e., pachyvessel) and choriocapillaris attenuation is well observed by OCT B-scans, especially ones that use a special charge coupled device or long-wave length light source such as EDI or swept-source (SS) OCT [2, 3, 6, 7]. Reported mean subfoveal choroidal thickness (SFCT) in eyes with pachychoroid was around 450 μm while the mean SFCT in normal eyes is around 277 to 332 μm [2, 8–10]. The proportion of Haller's layer to total choroidal thickness is 76.0 to 84.1%, while it has been reported to be around 55.0 to 70.0% in normal or typical age-related macular degeneration eyes [5, 8, 9, 11, 12]. These characteristic choroidal morphologies are used to differentiate pachychoroid and non-pachychoroid eyes by clinicians, and thereby, we reasoned that these could also be used to train an artificial intelligence model using a deep learning convolutional neural network design (CNN) to identify pachychoroid eyes.

Recently, AI has been applied to many areas of retinal imaging including grading of diabetic retinopathy (DR) and AMD, as well as in decision making for treatment [13–15]. Although distinguishing pachychoroid from non-pachychoroid could be a minor problem compared with DR and AMD grading, the identification of pachychoroid eyes in macular disease can assist clinicians to make more precise decisions for treatment. To assess the feasibility of automatic classification of pachychoroid, we investigated the performance of deep and shallow CNN models for detection of pachychoroid using OCT B-scan images in the current study.

Methods

This study was approved by the Institutional Review Board of Bucheon St. Mary's Hospital, which waived the need for written informed consent because of the study's retrospective design. The study was conducted in accordance with the tenets of the Declaration of Helsinki.

Subjects

One thousand ninety-eight OCT B-scan images from consecutive patients with macular diseases including CSC, PNV, PCV, and typical AMD between April 2016 and July 2020 were collected. All patients underwent high-definition (HD) OCT (DRI OCT Triton, Topcon Corporation, Tokyo, Japan) in the EDI mode and fluorescent angiography (Optos California P200DTx; Optos, Dunfermline, UK) at baseline to confirm their diagnosis.

The exclusion criteria for this study were as follows: (1) choroidal neovascularization other than AMD (e.g., punctate inner choroidopathy, vitelliform dystrophy), (2) history of previous treatment or scar at the retina (e.g., photodynamic therapy, laser photocoagulation, intraocular injections, periocular injections, and systemic injections), (3) high myopia (> − 6.00 diopters or axial length > 26 mm), (4) poor image quality (image quality < 7), and (5) large subretinal/preretinal hemorrhage or pigment epithelial detachment that could obscure the choroidal vascular image.

Labeling of images as pachychoroid (n = 1092) or non-pachychoroid (n = 806) was done using strict quantitative and qualitative criteria for multimodal imaging by two retina specialists. Confirmation of pachychoroid was based on criteria determined from thorough review of previous publications and comprised [16]: (1) subfoveal choroidal thickness (SFCT) ≥ 300 μm, (2) presence of attenuation of the inner choroid with dilated choroidal vessels (pachyvessel) under the diseased area on OCT B-scans, (3) presence of pachydrusen on fundus photography and OCT, and (4) choroidal vascular hyperpermeability on indocyanine green angiography (ICGA). These were the optional features used to confirm pachychoroid.

Image preparation, model training, and performance metrics

Each horizontal HD line OCT B-scan which crossed the fovea was saved as a JPEG file. All images were resized to 299 × 299 × 3 pixels. Models were trained using pretrained networks on MATLAB 2020a (MathWorks, Inc., Natick, MA, USA). For a CNN model, 80% of images were randomly selected for training and the remaining 20% were used for validation. In addition to the final accuracy returned from model training and validation, the performance of models was assessed using an independent test set.

The CNN architectures used in this study included AlexNet, VGG-16, ResNet50, Inception-v3, Inception-ResNet-v2, and Xception (Fig. 1). Selection of CNN architectures was based on a top 5 error rate reported previously for image classification and on previous publications on performances of these architectures in ophthalmologic images [17, 18]. All experiments were conducted on a laptop equipped with NVIDIA RTX 2060 and Intel i7 CPUs. Each model was trained for 30 epochs with a maximum of 1410 iterations. Final accuracy of the model was calculated after training and validation processes. Then, the performance of each model was evaluated for accuracy, precision, recall (sensitivity), specificity, F1 score, and kappa score using an independent test set that consisted of 50 non-pachychoroid and 50 pachychoroid images.

Statistics

Statistical analysis was performed using a commercial program (Statistical Package for the Social Sciences version 22.0.1 for Windows; IBM Corp., Armonk, NY, USA). t tests were used to compare demographics between groups, and the chi-squared test was used to compare categorical variables. Accuracy, precision, recall, specificity, and F1 score were calculated for each model. The kappa score means and standard deviations (SD) were used to determine the agreement between truth and each model. Continuous variables are presented as means ± SDs.

Results

Subject demographic and clinical characteristics

In total, 1898 images from 1898 eyes of 1470 patients (482 bilateral eyes) were included in the study. The mean age of the pachychoroid and non-pachychoroid groups was 61.19 ± 12.22 years and 73.86 ± 8.89 years, respectively (P < 0.001). The proportion of males was higher in the pachychoroid compared with non-pachychoroid group

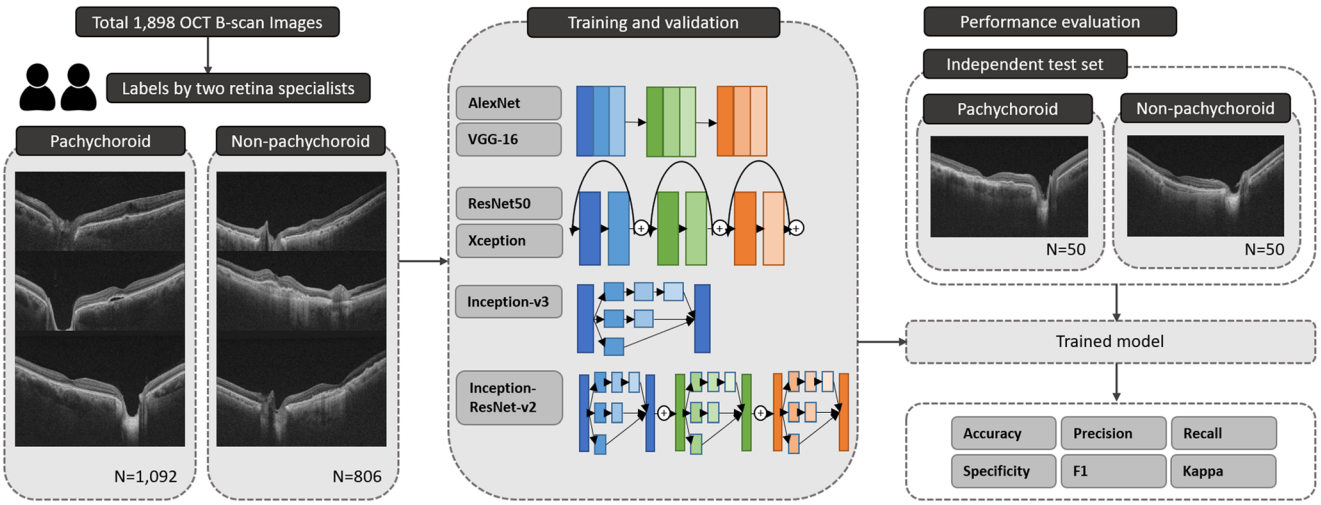

Fig. 1 Training, internal validation, and test of convolutional neural network (CNN) models. Fovea crossing horizontal optical coherence tomographic (OCT) B-scan images were obtained. The images were labeled either "pachychoroid" or "non-pachychoroid" by two independent graders. Each OCT image was scaled to 299 × 299 × 3 pixels for CNN training and trained with AlexNet, VGG-16, ResNet50, Inception-v3, Inception-ResNet-v2, and Xception architectures using MATLAB 2020a. From the dataset, 80% of the images were used for training, and the remaining 20% were used for validation. Trained CNN models were externally tested using an independent test set

(70.3% vs. 49.6%, $P < 0.001$). The mean SFCT was 407.82 ± 93.22 μm in pachychoroid eyes and 136.28 ± 67.95 μm in non-pachychoroid eyes ($P < 0.001$).

There was no difference in age, sex distribution, and SFCT between the dataset used for training-validation and the independent test set for both pachychoroid and non-pachychoroid groups (pachychoroid 60.98 ± 12.14 years vs. 63.48 ± 12.96 years, 70.9% vs. 65.4%, 409.54 ± 94.1 μm vs. 388.5 ± 80.97 μm, $P = 0.186$, 0.244, and 0.081, respectively; non-pachychoroid 73.8 ± 8.81 years vs. 75.16 ± 10.50; 50.1% vs. 40.0%; 137.19 ± 67.88 μm vs. 117.21 ± 67.54 μm, $P = 0.437$, 0.132, and 0.082, respectively).

Performance of the deep learning models

The final accuracy for the validation set was 57.52%, 57.52%, 96.31%, 95.25%, 93.40%, and 92.61% for AlexNet, VGG-16, ResNet50, Inception-v3, Inception-ResNet-v2, and Xception, respectively (Fig. 2). The relative time spent in model training was 0.42, 1.00, 0.78, 0.31, 0.99, and 0.82, respectively.

ResNet50, Inception-v3, Inception-ResNet-v2, and Xception were tested on the independent test set. Accuracy for each model on the test set was 78.00%, 86.00%, 90.00%, and 92.00%, for ResNet50, Inception-v3, Inception-ResNet-v2, and Xception, respectively. The precision and recall for each model were 1.00 and 0.56, 0.97 and 0.74, 0.95 and 0.84, and 0.92 and 0.92, respectively. The accuracy, precision, recall, specificity, F1 score, and kappa values for each model are summarized in Table 1.

Misclassified cases

The independent test set results showed that two pachychoroid images were misclassified as non-pachychoroid by all four models. Seven images were misclassified by at least three models of which one was non-pachychoroid misclassified as pachychoroid and 6 were pachychoroid misclassified as non-pachychoroid. The mean age was 71.75 ± 8.10 years, and the mean SFCT was 361.75 ± 81.33 μm in the misclassified pachychoroid eyes. Representatives of misclassified cases are shown in Fig. 3. Figure 3a is an OCT B-scan of a 78-year-old male. Although the image was labeled as non-pachychoroid due to an SFCT of 221 μm, there are dilated vessels under the abnormal RPE. Figure 3b and c are cases of pachychoroid that were misclassified as non-pachychoroid by all models. Both eyes did not show signs of typical AMD such as drusen or geographic atrophy, and SFCT was 318 μm and 327 μm, respectively; therefore, they were classified as pachychoroid. However, all four AI models classified these eyes as non-pachychoroid eyes.

Discussion

It has not been long since pachychoroid was recognized as a particular condition in macular diseases. Pachychoroid and typical AMD seem to differ in clinical features, genetics, natural course, and responsiveness to treatment [19–22]. Patients with pachychoroid are usually younger [5, 16, 20, 22]. In terms of treatment, a lower injection rate with a longer injection-free

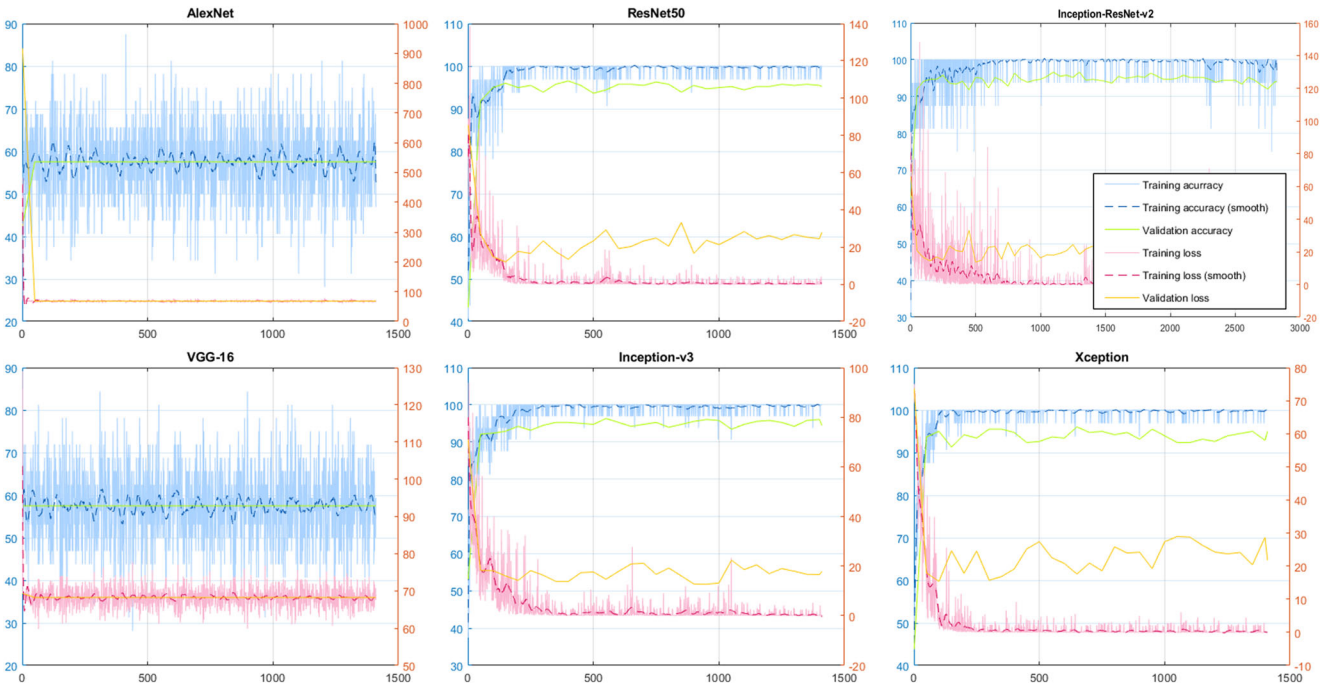

Fig. 2 Internal validation performance of each model. The final accuracy on the validation set was 57.52%, 57.52%, 96.31%, 95.25%, 93.40%, and 92.61% for AlexNet, VGG-16, ResNet50, Inception-v3, Inception-ResNet-v2, and Xception, respectively

Table 1 Classification performance of the deep convolutional neural network models on the test set

	ResNet50	Inception-v3	Inception-ResNet-v2	Xception
Accuracy	0.7800	0.8600	0.9000	0.9200
Precision	1.0000	0.9737	0.9545	0.9200
Recall	0.5600	0.7400	0.8400	0.9200
Specificity	1.0000	0.9800	0.9600	0.9200
F1 score	0.7179	0.8409	0.8936	0.9200
Kappa-mean	0.5600	0.7200	0.8000	0.8400
Kappa-SD	0.0744	0.0674	0.0600	0.0543

F1 score = 2×(precision × recall) / (precision + recall)

SD standard deviation

period was reported for PNV and PCV eyes with pachychoroid features compared with typical AMD [19, 23] [24]. Therefore, identification of pachychoroid is helpful in predicting disease prognosis by patient and in planning tailored treatment options and follow-up intervals. In this study, we assessed the efficacy of automated classification of pachychoroid and non-pachychoroid eyes using AI models trained with CNNs. CNN architectures including AlexNet, VGG-16, ResNet50, Inception-v3, Inception-ResNet-v2, and Xception were trained to automatically classify pachychoroid and non-pachychoroid eyes using OCT B-scan images of the fovea.

Self-validation of the trained model revealed an accuracy of 57.52–96.31%. Deep CNNs (ResNet-50, Inception-v3, Inception-ResNet-v2, and Xception) performed better than shallow CNNs (AlexNet and VGG-16). This result differs from that of AI models tested on chest radiographs by Bressem et al., which showed that an accurate classification of chest radiographs may be achieved with comparably shallow networks [25]. This may be due to the inherent capacity for image classification of these architectures, as demonstrated in previous ImageNet Large-Scale Visual Recognition Challenges [18]. Or there might be a difference in the feasibility of the architecture for OCT B-scans and chest radiographs, as OCT B-scans have lower complexity and pixel signals compared with chest radiograph images. More evidence from other studies supports better performance of deep

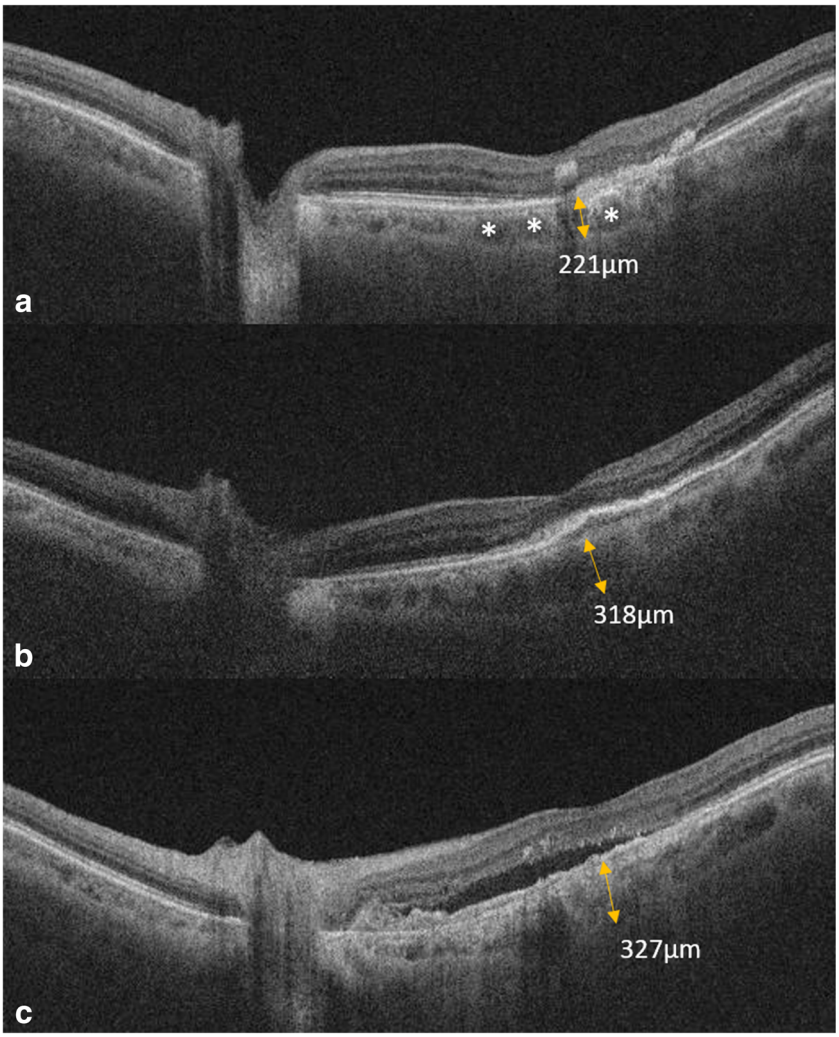

Fig. 3 Misclassified cases. **a** A case of non-pachychoroid misclassified as pachychoroid. Optical coherence tomography (OCT) B-scan from a 78-year-old male patient with type 1 neovascularization demonstrates a subfoveal choroidal thickness (SFCT) of 221 µm, but dilated Haller's vessels are seen under the lesion (asterisks). **b**, **c** Cases of pachychoroid misclassified as non-pachychoroid by all four models. The images are from 74-year-old and 73-year-old male patients. Although OCT shows increased vascular density with diffuse distribution of Haller's vessels, which are distinctive features of pachychoroid, a relatively thin SFCT (around 300) might have caused misclassification of these eyes as non-pachychoroid

rather than shallow CNNs for automated classification of OCT images [26–28].

These deeper CNNs also demonstrated good performance on the independent test set with an accuracy of 78.00–92.00%. The model trained with Xception had better performance in both precision and recall. Considering both performance and time spent in model training, Xception was the best architecture for building an AI model to classify pachychoroid using OCT B-scan images. For ResNet50, Inception-v3, and Inception-ResNet-v2, the final accuracies for validation were higher compared with the accuracies obtained with the independent test set. This may be explained by the possibility of overfitting. The training dataset might have been unnecessarily large for these architectures. Nonetheless, these models demonstrated good performance, as demonstrated by high precision, recall, specificity, F1 score, and kappa score on external validation, especially when using Inception-ResNet-v2.

In our previous study that investigated classification of pachychoroid using an auto-AI platform trained using ultra-widefield indocyanine green angiography (UWF ICGA), the precision and recall of the model was 89.19% [29]. AI models trained with OCT B-scan images in this study showed comparable results. UWF ICGA can reveal global changes of choroidal circulation such as dilation of vessels, choroidal vascular hyperpermeability, and congestion around vortex ampullae, while OCT B-scan images can emphasize detailed changes in choroidal layers focused on posterior pole [30, 31]. It is expected that the performance of the automatic classification could be improved by combining these two methods.

Misclassified cases demonstrated that errors caused by AI models are likely to occur in pachychoroid eyes from older patients with an SFCT around 300 μm. Choroidal thinning is a well-known aging process, and this does not exclude pachychoroid eyes [32]. It is suspected that these misclassified pachychoroid eyes might have had a thicker SFCT in their 1960s. The error that occurred in these eyes indicates that pachychoroid classification might be more difficult in older patients. These results also suggest that decreased model capacity to differentiate eyes can also happen with younger patients who have overlapping non-pachychoroid and pachychoroid features.

The limitations of this study include selection bias caused by excluding images with large subretinal/preretinal hemorrhage or PED. While these eyes often require proper treatment, this bias might cause high errors when classifying these eyes. Another important limitation might be that there was a significant difference in age and sex distribution between the pachychoroid and non-pachychoroid eye groups. However, as younger age and male prominence are well-established pachychoroid features that should also be observed in real life, this may not significantly affect clinical application of these models [22]. More importantly, the definition of pachychoroid may be controversial. We tried to minimize this ambiguity by specifying the quantitative value for SFCT in the definition of pachychoroid and by exploring multimodal images when setting ground truth. Further research involving multimodal images from many OCT machines and more retinal specialists are warranted to validate the results of the current investigation.

In this study, we evaluated the performance of CNN models for classification of pachychoroid and non-pachychoroid eyes using OCT B-scans. The results demonstrated that deeper CNN models, especially, Xception, could identify pachychoroid eyes with good performance. Analysis of errors in classification revealed that most occurred in PCV eyes with equivocal features. To the best of our knowledge, this is the first study to train CNN models on OCT B-scan for classification of pachychoroid eyes. We believe that this automated classification of pachychoroid features will improve treatment for patients with exudative maculopathies by assisting in precisely tailored treatment by patient.

Author contribution Contributions were as follows: N.Y.K. and H.R., preparation of data and data analysis; K.L., data analysis; J.H.L., collection of data and data analysis; W.K.L., conceptualization and preparation of data; J.B., conception and design of the study, writing manuscript text, preparing figures, collection and assembly of data, data analysis and interpretation, and supervision. All authors reviewed the manuscript.

Funding This work was supported by the Institute of Clinical Medicine Research of Bucheon St. Mary's Hospital, Research Fund, 2020.

Data Availability The datasets generated and/or analyzed during the current study are available from the corresponding author upon reasonable request.

Declarations

Ethics approval and consent to participate/publication This study was conducted in accordance with the tenets of the Declaration of Helsinki. The study was approved by the Institutional Review Board of Bucheon St. Mary's Hospital, which waived the need for written informed consent because of the study's retrospective design (HC19RESI0086).

Competing interests The authors declare that they have no competing interests.

References

1. Guyer DR, Yannuzzi LA, Slakter JS, Sorenson JA, Ho A, Orlock D (1994) Digital indocyanine green videoangiography of central serous chorioretinopathy. Arch Ophthalmol 112:1057–1062
2. Warrow DJ, Hoang QV, Freund KB (2013) Pachychoroid pigment epitheliopathy. Retina 33:1659–1672. https://doi.org/10.1097/IAE.0b013e3182953df4
3. Pang CE, Freund KB (2015) Pachychoroid neovasculopathy. Retina 35:1–9. https://doi.org/10.1097/IAE.0000000000000331
4. Fung AT, Yannuzzi LA, Freund KB (2012) Type 1 (sub-retinal pigment epithelial) neovascularization in central serous chorioretinopathy masquerading as neovascular age-related

macular degeneration. Retina 32:1829–1837. https://doi.org/10.1097/IAE.0b013e3182680a66
5. Lee WK, Baek J, Dansingani KK, Lee JH, Freund KB (2016) Choroidal morphology in eyes with polypoidal choroidal vasculopathy and normal or subnormal subfoveal choroidal thickness. Retina 36(Suppl 1):S73–s82. https://doi.org/10.1097/iae.0000000000001346
6. Dansingani KK, Balaratnasingam C, Naysan J, Freund KB (2016) En face imaging of pachychoroid spectrum disorders with swept-source optical coherence tomography. Retina 36:499–516. https://doi.org/10.1097/IAE.0000000000000742
7. Spaide RF, Koizumi H, Pozzoni MC (2008) Enhanced depth imaging spectral-domain optical coherence tomography. Am J Ophthalmol 146:496–500. https://doi.org/10.1016/j.ajo.2008.05.032
8. Zhao J, Wang YX, Zhang Q, Wei WB, Xu L, Jonas JB (2018) Macular choroidal small-vessel layer, Sattler's layer and Haller's layer thicknesses: the Beijing Eye Study. Sci Rep 8:4411. https://doi.org/10.1038/s41598-018-22745-4
9. Chung YR, Kim JW, Choi SY, Park SW, Kim JH, Lee K (2018) Subfoveal choroidal thickness and vascular diameter in active and resolved central serous chorioretinopathy. Retina 38:102–107. https://doi.org/10.1097/iae.0000000000001502
10. Chung SE, Kang SW, Lee JH, Kim YT (2011) Choroidal thickness in polypoidal choroidal vasculopathy and exudative age-related macular degeneration. Ophthalmology 118:840–845. https://doi.org/10.1016/j.ophtha.2010.09.012
11. Lai K, Zhou L, Zhong X, Huang C, Gong Y, Xu F, Ma L, Chen G, Cheng L, Lu L, Jin C (2018) Morphological difference of choroidal vasculature between polypoidal choroidal vasculopathy and neovascular AMD on OCT: from the perspective of pachychoroid. Ophthalmic Surg Lasers Imaging Retina 49:e114–e121. https://doi.org/10.3928/23258160-20181002-13
12. Flores-Moreno I, Arcos-Villegas G, Sastre M, Ruiz-Medrano J, Arias-Barquet L, Duker JS, Ruiz-Moreno JM (2020) Changes in choriocapillaris, Sattler, and Haller layer thicknesses in central serous chorioretinopathy after half-fluence photodynamic therapy. Retina. https://doi.org/10.1097/iae.0000000000002764
13. Burlina PM, Joshi N, Pekala M, Pacheco KD, Freund DE, Bressler NM (2017) Automated grading of age-related macular degeneration from color fundus images using deep convolutional neural networks. JAMA Ophthalmol 135:1170–1176. https://doi.org/10.1001/jamaophthalmol.2017.3782
14. Gargeya R, Leng T (2017) Automated identification of diabetic retinopathy using deep learning. Ophthalmology 124:962–969. https://doi.org/10.1016/j.ophtha.2017.02.008
15. Ting DSW, Cheung CY, Lim G, Tan GSW, Quang ND, Gan A, Hamzah H, Garcia-Franco R, San Yeo IY, Lee SY, Wong EYM, Sabanayagam C, Baskaran M, Ibrahim F, Tan NC, Finkelstein EA, Lamoureux EL, Wong IY, Bressler NM, Sivaprasad S, Varma R, Jonas JB, He MG, Cheng CY, Cheung GCM, Aung T, Hsu W, Lee ML, Wong TY (2017) Development and validation of a deep learning system for diabetic retinopathy and related eye diseases using retinal images from multiethnic populations with diabetes. JAMA 318:2211–2223. https://doi.org/10.1001/jama.2017.18152
16. Yanagi Y (2020) Pachychoroid disease: a new perspective on exudative maculopathy. Jpn J Ophthalmol. https://doi.org/10.1007/s10384-020-00740-5
17. Ting DSW, Pasquale LR, Peng L, Campbell JP, Lee AY, Raman R, Tan GSW, Schmetterer L, Keane PA, Wong TY (2019) Artificial intelligence and deep learning in ophthalmology. Br J Ophthalmol 103:167–175. https://doi.org/10.1136/bjophthalmol-2018-313173
18. Véstias MP (2019) A survey of convolutional neural networks on edge with reconfigurable computing. Algorithms 12:154. https://doi.org/10.3390/a12080154
19. Baek J, Lee JH, Lee K, Chung BJ, Lee WK (2019) Clinical outcome of polypoidal choroidal vasculopathy/aneurysmal type 1 neovascularization according to choroidal vascular morphology. Retina. https://doi.org/10.1097/IAE.0000000000002723
20. Chang YC, Cheng CK (2019) Difference between pachychoroid and nonpachychoroid polypoidal choroidal vasculopathy and their response to anti-vascular endothelial growth factor therapy. Retina. https://doi.org/10.1097/IAE.0000000000002583
21. Forte R, Coscas F, Serra R, Cabral D, Colantuono D, Souied EH (2019) Long-term follow-up of quiescent choroidal neovascularisation associated with age-related macular degeneration or pachychoroid disease. Br J Ophthalmol. https://doi.org/10.1136/bjophthalmol-2019-315189
22. Miyake M, Ooto S, Yamashiro K, Takahashi A, Yoshikawa M, Akagi-Kurashige Y, Ueda-Arakawa N, Oishi A, Nakanishi H, Tamura H, Tsujikawa A, Yoshimura N (2015) Pachychoroid neovasculopathy and age-related macular degeneration. Sci Rep 5:16204. https://doi.org/10.1038/srep16204
23. Morimoto M, Matsumoto H, Mimura K, Akiyama H (2017) Two-year results of a treat-and-extend regimen with aflibercept for polypoidal choroidal vasculopathy. Graefes Arch Clin Exp Ophthalmol 255:1891–1897. https://doi.org/10.1007/s00417-017-3718-6
24. Matsumoto H, Hiroe T, Morimoto M, Mimura K, Ito A, Akiyama H (2018) Efficacy of treat-and-extend regimen with aflibercept for pachychoroid neovasculopathy and type 1 neovascular age-related macular degeneration. Jpn J Ophthalmol 62:144–150. https://doi.org/10.1007/s10384-018-0562-0
25. Bressem KK, Adams LC, Erxleben C, Hamm B, Niehues SM, Vahldiek JL (2020) Comparing different deep learning architectures for classification of chest radiographs. Sci Rep 10:13590. https://doi.org/10.1038/s41598-020-70479-z
26. Feng D, Chen X, Zhou Z, Liu H, Wang Y, Bai L, Zhang S, Mou X (2020) A preliminary study of predicting effectiveness of anti-VEGF injection using OCT images based on deep learning. Annu Int Conf IEEE Eng Med Biol Soc 2020:5428–5431. https://doi.org/10.1109/embc44109.2020.9176743
27. Yu C, Xie S, Niu S, Ji Z, Fan W, Yuan S, Liu Q, Chen Q (2019) Hyper-reflective foci segmentation in SD-OCT retinal images with diabetic retinopathy using deep convolutional neural networks. Med Phys 46:4502–4519. https://doi.org/10.1002/mp.13728
28. Park K, Kim J, Kim S, Shin J (2020) Prediction of visual field from swept-source optical coherence tomography using deep learning algorithms. Graefes Arch Clin Exp Ophthalmol. https://doi.org/10.1007/s00417-020-04909-z
29. Kim IK, Lee K, Park JH, Baek J, Lee WK (2020) Classification of pachychoroid disease on ultrawide-field indocyanine green angiography using auto-machine learning platform. Br J Ophthalmol. https://doi.org/10.1136/bjophthalmol-2020-316108
30. Pang CE, Shah VP, Sarraf D, Freund KB (2014) Ultra-widefield imaging with autofluorescence and indocyanine green angiography in central serous chorioretinopathy. Am J Ophthalmol 158:362–371.e362. https://doi.org/10.1016/j.ajo.2014.04.021
31. Lee A, Ra H, Baek J (2020) Choroidal vascular densities of macular disease on ultra-widefield indocyanine green angiography. Graefes Arch Clin Exp Ophthalmol 258:1921–1929. https://doi.org/10.1007/s00417-020-04772-y
32. Chirco KR, Sohn EH, Stone EM, Tucker BA, Mullins RF (2017) Structural and molecular changes in the aging choroid: implications for age-related macular degeneration. Eye (Lond) 31:10–25. https://doi.org/10.1038/eye.2016.216

Publisher's Note Springer Nature remains neutral with regard to jurisdictional claims in published maps and institutional affiliations.